

A low-density hot Jupiter in a near-aligned, 4.5-day orbit around a $V = 10.8$, F5V star

D. R. ANDERSON,¹ F. BOUCHY,² D. J. A. BROWN,^{3,4} A. BURDANOV,⁵ A. COLLIER CAMERON,⁶ L. DELREZ,^{5,7} M. GILLON,⁵ C. HELLIER,¹ E. JEHIN,⁵
M. LENDL,^{2,8} P. F. L. MAXTED,¹ L. D. NIELSEN,² F. PEPE,² D. POLLACCO,^{3,4} D. QUELOZ,^{2,7} D. SÉGRANSAN,² B. SMALLEY,¹ L. Y. TEMPLE,¹
A. H. M. J. TRIAUD,⁹ S. UDRY,² AND R. G. WEST^{3,4}

¹*Astrophysics Group, Keele University, Staffordshire ST5 5BG, UK*

²*Observatoire de Genève, Université de Genève, 51 Chemin des Maillettes, 1290 Sauverny, Switzerland*

³*Department of Physics, University of Warwick, Coventry CV4 7AL, UK*

⁴*Centre for Exoplanets and Habitability, University of Warwick, Gibbet Hill Road, Coventry CV4 7AL, UK*

⁵*Space sciences, Technologies and Astrophysics Research (STAR) Institute, Université de Liège 1, Belgium*

⁶*SUPA, School of Physics and Astronomy, University of St. Andrews, North Haugh, Fife KY16 9SS, UK*

⁷*Cavendish Laboratory, J J Thomson Avenue, Cambridge CB3 0HE, UK*

⁸*Space Research Institute, Austrian Academy of Sciences, Schmiedlstr. 6, 8042 Graz, Austria*

⁹*School of Physics & Astronomy, University of Birmingham, Edgbaston, Birmingham, B15 2TT, UK*

(Received September 20, 2018)

ABSTRACT

We report the independent discovery and characterisation of a hot Jupiter in a 4.5-d, transiting orbit around the star TYC 7282-1298-1 ($V = 10.8$, F5V). The planet has been pursued by the NGTS team as NGTS-2b and by ourselves as WASP-179b. We characterised the system using a combination of photometry from WASP-South and TRAPPIST-South, and spectra from CORALIE (around the orbit) and HARPS (through the transit). We find the planet's orbit to be nearly aligned with its star's spin. From a detection of the Rossiter-McLaughlin effect, we measure a projected stellar obliquity of $\lambda = -19 \pm 6^\circ$. From line-profile tomography of the same spectra, we measure $\lambda = -11 \pm 5^\circ$. We find the planet to have a low density ($M_P = 0.67 \pm 0.09 M_{\text{Jup}}$, $R_P = 1.54 \pm 0.06 R_{\text{Jup}}$), which, along with its moderately bright host star, makes it a good target for transmission spectroscopy. We find a lower stellar mass ($M_* = 1.30 \pm 0.07 M_\odot$) than reported by the NGTS team ($M_* = 1.64 \pm 0.21 M_\odot$), though the difference is only 1.5σ .

Keywords: planets and satellites: individual (WASP-179b, NGTS-2b) — stars: individual (TYC 7282-1298-1, WASP-179, NGTS-2)

1. INTRODUCTION

Ground-based transit surveys are well matched to finding ‘hot Jupiters’, gas-giant planets in close orbits of a few days. Such systems are among the best targets for characterisation of planetary atmospheres, particularly when the host star is relatively bright and when the planet is bloated (e.g. Wyttenbach et al. 2017; Kreidberg et al. 2018; Spake et al. 2018).

Raynard et al. (2018), hereafter R18, recently reported the discovery and characterisation of a hot Jupiter in a transiting orbit around the star TYC 7282-1298-1. Having detected transits of the star using the Next Generation Transit Survey (NGTS; Wheatley et al. 2018), R18 confirmed the exis-

tence of the planet and derived the system's parameters using a combination of the transit lightcurves from NGTS and radial velocities around the orbit calculated from HARPS spectra (Pepe et al. 2002). R18 reported NGTS-2b to be a low-density planet ($M_P = 0.74 \pm 0.13 M_{\text{Jup}}$, $R_P = 1.595 \pm 0.046 R_{\text{Jup}}$) in a 4.51-d orbit around a rapidly rotating ($v_* \sin i_* = 15.2 \pm 0.8 \text{ km s}^{-1}$) F5V star.

The WASP transit survey (Pollacco et al. 2006) had also been following the star since finding a transit signal and adopting it as a candidate in 2013. We present here an independent discovery and characterisation of the system, which we also designate WASP-179 (noting that many planetary systems have been given designations by more than one transit team; e.g. Labadie-Bartz et al. 2018). Being rare, the reporting of such an independent discovery is an important verification of the planet and a validation of the techniques of the respective surveys.

In addition to transit photometry and spectra around the orbit, we report spectra taken through a transit of the planet, from which we derive the projected stellar obliquity (projected spin-orbit angle, λ). Stellar obliquity is considered a diagnostic for the mechanisms via which hot Jupiters migrated to their current orbits (see Dawson & Johnson 2018 for a recent review on the origins of hot Jupiters).

2. OBSERVATIONS

We observed WASP-179 ($V = 10.8$) during 2006–2008 and during 2011–2014 with the WASP-South facility (Fig. 1, top panel; Pollacco et al. 2006), and identified it as a candidate transiting-planet system using the techniques described in Collier Cameron et al. (2006, 2007). We conducted photometric follow-up using the 0.6-m TRAPPIST-South imager (Gillon et al. 2011; Jehin et al. 2011) and spectroscopic follow-up using both CORALIE on the 1.2-m Euler-Swiss telescope (Queloz et al. 2000) and HARPS on the 3.6-m ESO telescope (Pepe et al. 2002).

From the TRAPPIST photometry we confirmed that the periodic photometric dip is on-target and that the transit ephemeris and shape are consistent with the WASP-South photometry (Fig. 1, second panel). An unresolved star can impact the determination of the system parameters by diluting the transits (e.g. Evans et al. 2016; Günther et al. 2018), but the Gaia DR2 (Gaia Collaboration et al. 2018) excludes nearby sources beyond its angular resolution limit of $0.4''$. We computed radial-velocity (RV) measurements from the CORALIE and HARPS spectra by weighted cross-correlation with a G2 binary mask (Baranne et al. 1996; Pepe et al. 2002). We detected a sinusoidal variation in the CORALIE RVs that phases with the WASP ephemeris and which has a semi-amplitude consistent with a planetary mass companion (Fig. 1, third panel). We timed the HARPS observations to coincide with a transit, aiming to measure the projected stellar obliquity via the Rossiter-McLaughlin (RM) effect (e.g. Albrecht et al. 2012). Using an exposure time of 10 min, we took 32 spectra in high-accuracy mode (HAM) through the transit on the night of 2018 Mar 27 (Fig. 1, bottom panel). The sequence began after ingress as the telescope was previously occupied by technical intervention. To more precisely measure the orbital eccentricity and the amplitude of the stellar reflex motion we included in our analysis the 16 HARPS RVs from Raynard et al. (2018): ten spectra were obtained in HAM (four with 20-min exposures and six with 40-min exposures) and six spectra were obtained in high-efficiency mode (EGGS) with 20-min exposures. See Table 1 for a summary of the observations used in this paper. See Table 2 and Table 3 for the RVs and photometry, respectively.

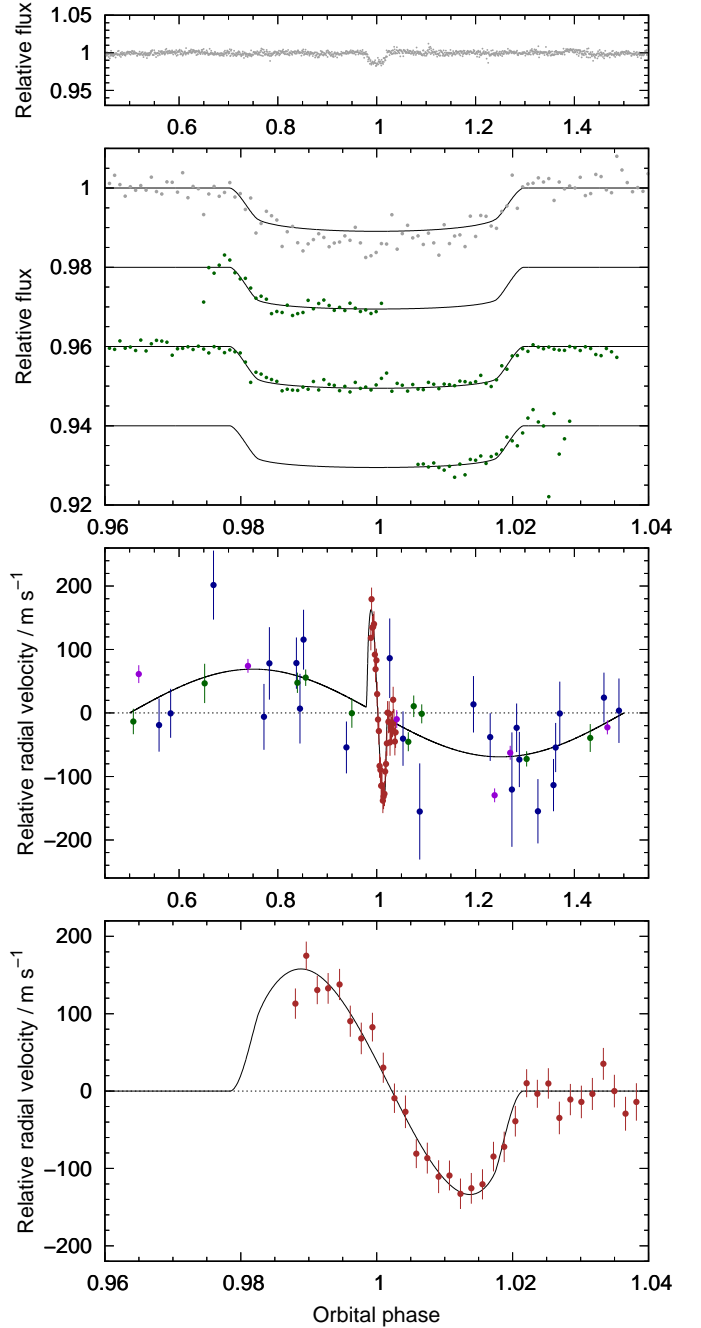


Figure 1. WASP-179b discovery data. *Top panel:* WASP-South lightcurve folded on the transit ephemeris. *Second panel:* Transit lightcurves from WASP-South (grey) and TRAPPIST (green), offset for clarity, binned with a bin width equivalent to five minutes, and plotted chronologically with the most recent at the bottom. The best-fitting transit model is superimposed. *Third panel:* The CORALIE (blue) and HARPS (HAM = green, EGGS = violet, RM = brown) RVs with the best-fitting orbital and RM models. *Bottom panel:* The apparent radial-velocity anomaly illustrated by HARPS RVs during transit, together with the best-fitting RM effect model. The best-fitting orbital model has been subtracted.

Table 1. Summary of observations

Facility	Date ^a	N_{obs}	Notes ^b
<i>Photometry</i>			
WASP-South	2006 May–2014 Aug	77 549	400–700 nm
TRAPPIST-South	2015 Apr 23	538	$I+z$
TRAPPIST-South	2018 Apr 14	1 366	$I+z$
TRAPPIST-South	2018 Apr 23	400	$I+z$
<i>Spectroscopy</i>			
Euler/CORALIE	2015 Mar–2017 Apr	23	orbit
ESO3.6/HARPS ^c	2017 Jul–2018 Mar	16	orbit
ESO3.6/HARPS	2018 Mar 27	32	transit

^aThe dates are ‘night beginning’.

^bFor the photometry datasets, we state which filter was used. For the spectroscopy datasets, we indicate whether the data cover the orbit or the transit.

^cFrom Raynard et al. (2018).

Table 2. Photometry

BJD(UTC) –2450000 (day)	Rel. flux, F	σ_F	Imager	Set
3860.389988	1.005491	0.005538	WASP-South	1
3860.390324	0.994179	0.005506	WASP-South	1
...				
7136.476710	0.995092	0.010803	TRAPPIST-S	2
7136.476940	0.990677	0.010697	TRAPPIST-S	2
...				

The flux values are differential and normalised to the out-of-transit levels. The uncertainties are the formal errors (i.e. they have not been rescaled). This table is available in its entirety via the CDS.

We checked for a correlation between RV and bisector span, which can indicate that an RV signal is the result of stellar activity (Queloz et al. 2001), or that an RV signal and a transit signal are both due to a blended eclipsing binary (Torres et al. 2004). There is no significant correlation (Fig. 2). Further, the detection of the RM effect and the nature of the trace in the Doppler tomogram (Section 4) conclusively prove that the photometric and spectroscopic signals are induced by a planet (Collier Cameron et al. 2010b; Jenkins et al. 2010).

3. STELLAR ANALYSIS

We co-added the individual HARPS spectra from the night of 2018 Mar 27 to obtain an average signal-to-noise of 150:1.

Table 3. Radial velocities

BJD(UTC) –2450000 (day)	RV (km s^{-1})	σ_{RV} (km s^{-1})	BS (km s^{-1})	Spectrograph
7111.734763	–26.3518	0.0508	0.0055	CORALIE
7175.700117	–26.1538	0.0544	0.1546	CORALIE
...				
8205.671957	–26.2426	0.0195	–0.0268	HARPS
8205.679191	–26.1815	0.0183	–0.1014	HARPS
...				

Uncertainties are the formal errors (i.e. with no added jitter). The uncertainty on bisector span (BS) is $2\sigma_{\text{RV}}$. This table is available in its entirety via the CDS.

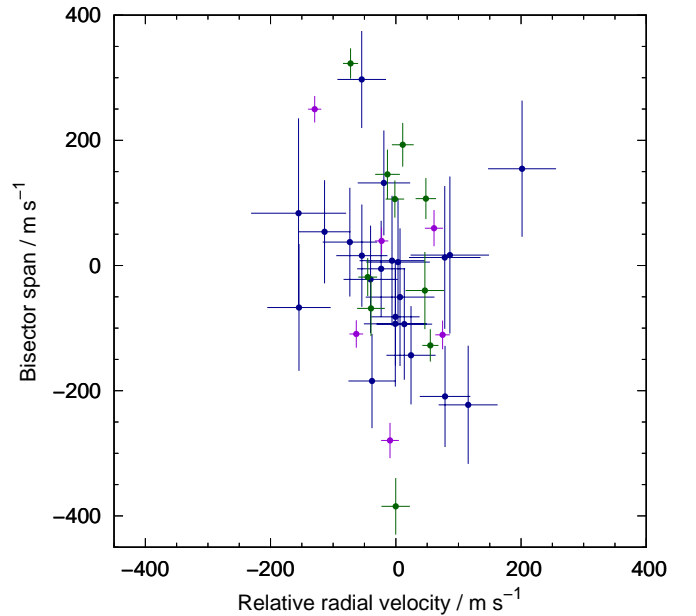


Figure 2. Bisector span versus radial velocity (CORALIE = blue symbols; HARPS HAM = green symbols; HARPS EGGS = violet symbols). The weak correlation is not statistically significant. For CORALIE: $r_{\text{weighted}} = -0.29$, with weight = σ_{RV}^{-1} ; p -value = 0.17. For HARPS: $r_{\text{weighted}} = -0.40$; p -value = 0.12. Combined: $r_{\text{weighted}} = -0.36$; p -value = 0.03. We omit the HARPS data taken through the transit as they are affected by the RM effect.

We performed a spectral analysis using the procedures detailed in Doyle et al. (2013) to obtain stellar effective temperature, surface gravity, metallicity, and projected rotation speed. We calculated macroturbulence using a slight extrapolation of the calibration of Doyle et al. (2014) and we calculated microturbulence using the calibration of Bruntt et al. (2012). We do not detect lithium in the spectra. The results of the spectral analysis are given in Table 4.

We searched the WASP-South lightcurves for modulation, as may result from the combination of stellar rotation and

Table 4. Stellar parameters

Parameter	Symbol	Value	Unit
Constellation	...	Centaurus	...
Right Ascension (J2000)	...	14 ^h 20 ^m 29 ^s .49	...
Declination (J2000)	...	-31° 12' 07.4	...
Tycho-2 V_{mag}	...	10.8	...
2MASS K_{mag}	...	9.8	...
Spectral type ^a	...	F5V	...
Stellar effective temperature	T_{eff}	6450 ± 50	K
Stellar mass	M_*	1.302 ± 0.034	M_{\odot}
Stellar radius (IRFM)	$R_{*,\text{IRFM}}$	1.62 ± 0.09	R_{\odot}
Stellar surface gravity	$\log g_*$	4.1 ± 0.1	[cgs]
Stellar metallicity ^b	[Fe/H]	-0.09 ± 0.09	...
Stellar luminosity	$\log(M_*/M_{\odot})$	0.691 ± 0.050	...
Proj. stellar rotation speed	$v \sin i_{*,\text{spec}}$	14.8 ± 1.0	km s ⁻¹
Macroturbulence	v_{mac}	6.4 ± 0.7	km s ⁻¹
Microturbulence	ξ_t	1.6 ± 0.1	km s ⁻¹
Reddening	$E(B - V)$	0.068	...
Distance	d	350 ± 11	pc
Age	τ	2.7 ± 0.2	Gyr

^a Spectral type estimated using the MKCLASS spectral classification code of Gray & Corbally (2014).

^b Iron abundance is relative to the solar value of Asplund et al. (2009).

magnetic activity, using the method of Maxted et al. (2011). We found no convincing signal, unsurprising for an F5V star, and place an upper limit of ~ 1 mmag on the amplitude of any sinusoidal signal.

We calculated the distance to WASP-179 ($d = 350 \pm 11$ pc) using a parallax of 2.861 ± 0.096 mas, which is the Gaia DR2 parallax with the correction suggested by Stassun & Torres (2018) applied. We calculated the effective temperature ($T_{\text{eff,IRFM}} = 6770 \pm 150$ K) and angular diameter ($\theta = 0.043 \pm 0.002$ mas) of the star using the infrared flux method (IRFM) of Blackwell & Shallis (1977), assuming reddening of $E(B - V) = 0.068$ from dust maps (Schlafly & Finkbeiner 2011). We thus calculated its luminosity ($\log(L/L_{\odot}) = 0.691 \pm 0.050$) and its radius ($R_{*,\text{IRFM}} = 1.62 \pm 0.09 R_{\odot}$), which is consistent with the value of R18 ($1.70 \pm 0.05 R_{\odot}$). If instead we use the non-corrected Gaia DR2 parallax (2.779 ± 0.063 mas) then we obtain: $d = 360 \pm 8$ pc, $R_{*,\text{IRFM}} = 1.67 \pm 0.09 R_{\odot}$, and $\log(L/L_{\odot}) = 0.716 \pm 0.045$.

Though we can measure stellar density, ρ_* , directly from the transit lightcurves, we require a constraint on stellar mass M_* , or radius R_* , for a full characterisation of the system. We inferred $M_* = 1.302 \pm 0.034 M_{\odot}$ and age $\tau = 2.7 \pm 0.2$ Gyr using the BAGEMASS stellar evolution MCMC code of

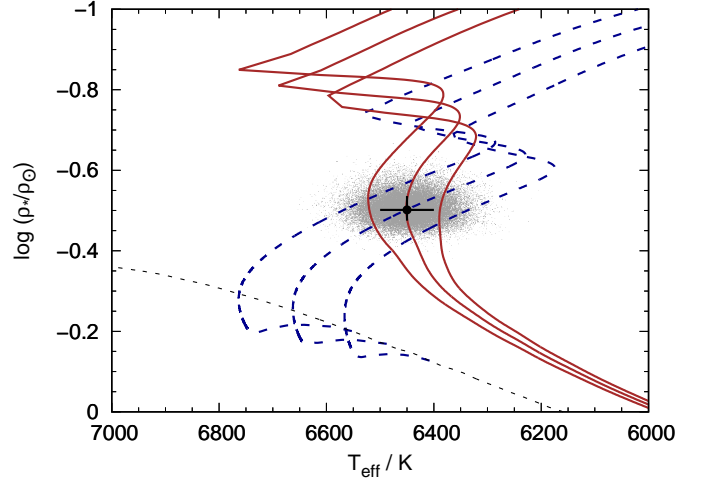


Figure 3. A modified Hertzsprung-Russell diagram showing the results of the BAGEMASS MCMC analysis for WASP-179. The grey dots are the steps in the Markov chain. The dotted line (black) is the ZAMS. The solid lines (brown) are isochrones for $\tau = 2.7 \pm 0.2$ Gyr. The dashed lines (blue) are evolutionary tracks for $M_* = 1.302 \pm 0.034 M_{\odot}$. The black point with error bars are the values of T_{eff} and ρ_* measured from the spectra and the transit lightcurves, respectively.

Maxted et al. (2015) with input of the values of ρ_* from an initial MCMC analysis (see Section 4) and T_{eff} and [Fe/H] from the spectral analysis (Fig. 3). We conservatively inflated the error bar by a factor of 2 to place a Gaussian prior on M_* ($1.30 \pm 0.07 M_{\odot}$) in our final MCMC analysis. We note that we derive a value of R_* ($1.62 \pm 0.06 R_{\odot}$) from our final MCMC that is consistent with the value that we obtained from the IRFM and Gaia parallax ($1.62 \pm 0.09 R_{\odot}$), which we could have used to place a Gaussian prior on R_* instead.

4. STELLAR OBLIQUITY AND SYSTEM PARAMETERS FROM AN MCMC ANALYSIS

We determined the system parameters from a simultaneous fit to the transit lightcurves and the radial velocities using the current version of the Markov-chain Monte Carlo (MCMC) code presented in Collier Cameron et al. (2007) and described further in Anderson et al. (2015). We modelled the RM effect using the formulation of Hirano et al. (2011).

When we fit for an eccentric orbit we obtained $e = 0.05^{+0.04}_{-0.03}$, with a 2- σ upper limit of $e < 0.14$. In the absence of evidence to the contrary we adopt a circular orbit, as advocated in Anderson et al. (2012). We accounted for stellar noise in the RV measurements by adding in quadrature with the formal RV uncertainties the level of ‘jitter’ required to achieve $\chi^2_{\text{reduced}} = 1$. The jitter values were: 32 m s⁻¹ (CORALIE RVs), 18.4 m s⁻¹ (HARPS HAM RVs of R18), 36.6 m s⁻¹ (HARPS EGGS RVs of R18). No jitter was re-

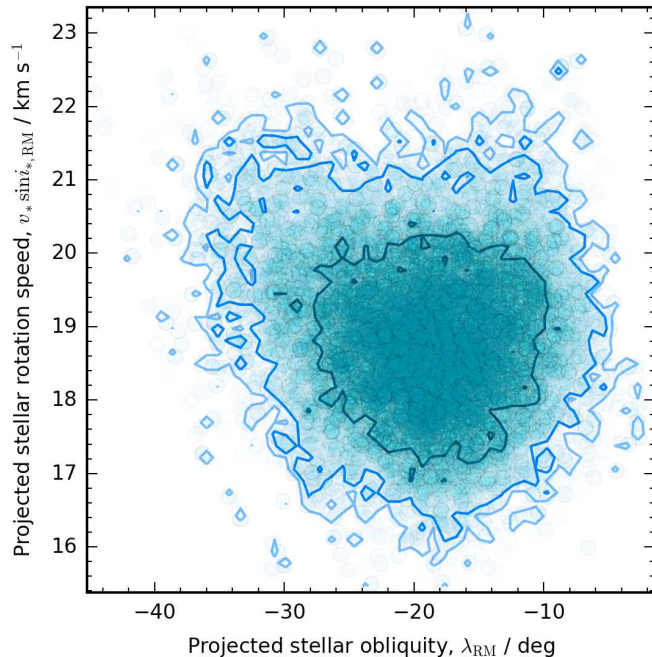


Figure 4. The MCMC posterior distributions of $v_* \sin i_{*,\text{RM}}$ and λ_{RM} when fitting the RM effect. The contours are the 68, 95 and 99 per cent confidence intervals.

quired for our HARPS RM RVs. To account for instrumental and astrophysical offsets, we partitioned the four RV datasets and fit a separate systemic velocity to each of them. When fit separately, our CORALIE RVs suggest a slightly larger stellar reflex velocity semi-amplitude ($K_1 = 72 \pm 16 \text{ m s}^{-1}$) than do the HARPS RVs of R18 ($K_1 = 68 \pm 11 \text{ m s}^{-1}$). When we analyse all of the RVs together we get $K_1 = 69.1 \pm 8.9 \text{ m s}^{-1}$. These values are consistent both with each other and with the value of R18 ($K_1 = 65.8 \pm 9.3 \text{ m s}^{-1}$).

We present the median values and $1\text{-}\sigma$ limits on the system parameters from our final MCMC analysis in Table 5. We plot the best fits to the RVs and the transit lightcurves in Fig. 1. The posterior distributions of the projected stellar rotation speed and the projected stellar obliquity indicate no degeneracy (Fig. 4), which is a result of the impact parameter being significantly non-zero ($b = 0.317 \pm 0.089$). We see no evidence in the RV residuals for an additional body in the system (Fig. 5). When we fit for a linear trend in RV, we obtained $\dot{\gamma} = -10 \pm 17 \text{ m s}^{-1} \text{ yr}^{-1}$.¹

We performed an additional fit in which we measured the stellar obliquity using line-profile tomography instead of the RM effect (so we omitted the HARPS RVs taken on the transit night of 2018 Mar 27). We modelled the average stellar line profiles (cross-correlation functions, or

CCFs) and the planet’s Doppler shadow using the method presented in Collier Cameron et al. (2010a) and used again in Collier Cameron et al. (2010b), Brown et al. (2012, 2017), and Temple et al. (2017, 2018). We plot the tomogram (i.e. the residual map of the CCF time-series) both before and after removal of the planet model in Fig. 6. The fitted parameters were the projected stellar rotation speed $v_* \sin i_{*,\text{DT}}$, the projected stellar obliquity λ_{DT} , the impact parameter b_{DT} , the FWHM of the line-profile perturbation due to the planet v_{FWHM} , and the centre-of-mass velocity γ_{DT} . We give the values of those parameters in Table 5. We omit the values of the other parameters as, depending mostly on the transit lightcurves and radial-velocity data, they are fully consistent between the two analyses.

5. DISCUSSION

We have reported the characterisation of WASP-179b (NGTS-2b), a hot Jupiter ($M_{\text{P}} = 0.67 \pm 0.09 M_{\text{Jup}}$, $R_{\text{P}} = 1.54 \pm 0.06 R_{\text{Jup}}$) in a 4.51-d orbit around a $V = 10.8$, F5V star. As a low-density planet orbiting a relatively bright star, WASP-179b is a good target for atmospheric characterisation via transmission spectroscopy (e.g. Spake et al. 2018). We predict an atmospheric scale height of $\sim 1050 \text{ km}$ and a transmission signal similar in amplitude to that of WASP-139b (Hellier et al. 2017) and one tenth that of WASP-107b (see table 4 of Anderson et al. 2017), which are both bloated super-Neptunes.

From an observation of the RM effect, we find the planet to be in a prograde orbit, with a slight misalignment between the planet’s orbital axis and the star’s spin axis ($\lambda_{\text{RM}} = -19 \pm 6^\circ$). We find this to be corroborated by our tomographic analysis of the same transit spectra ($\lambda_{\text{RM}} = -11 \pm 5^\circ$). The near-alignment of the system and the near-circular orbit ($e = 0.05^{+0.04}_{-0.03}$; $e < 0.14$ at 2σ) are compatible with WASP-179b having arrived in its current orbit via disc migration (see, e.g. Dawson & Johnson 2018). High-eccentricity migration (e.g. Petrovich 2015) is not ruled out, however, as we calculate a circularisation timescale of just 20 Myr (e.g. Jackson et al. 2008; assuming $Q'_p = 10^5$). We obtain a larger estimate of the stellar rotation speed from fitting the RM effect with the Hirano model than we do from both our tomographic and spectral analyses ($v_* \sin i_{*,\text{RM}} = 18.9 \pm 1.1 \text{ km s}^{-1}$, $v_* \sin i_{*,\text{DT}} = 15.91 \pm 0.49 \text{ km s}^{-1}$, $v_* \sin i_{*,\text{spec}} = 14.8 \pm 1.0 \text{ km s}^{-1}$), as was observed previously for other systems by Brown et al. (2017).

The system parameters reported by R18 differ somewhat to those presented herein. Most notably, their stellar mass ($M_* = 1.64 \pm 0.21 M_\odot$) is a little higher than ours ($M_* = 1.30 \pm 0.07 M_\odot$). Thus we find a smaller planetary mass than do R18: $M_{\text{P}} = 0.67 \pm 0.09 M_{\text{Jup}}$ compared to $M_{\text{P}} = 0.74 \pm 0.13 M_{\text{Jup}}$ (the difference is smaller than suggested by M_* as we measured a larger stellar reflex velocity ampli-

¹ We excluded the RVs from the transit night, except for the final two RVs, which we fit together with the 10 HARPS HAM RVs of R18.

Table 5. System parameters from an MCMC analysis

Parameter	Symbol	Value	Unit
<i>MCMC Gaussian priors</i>			
Stellar mass	M_*	1.30 ± 0.07	M_\odot
Stellar effective temperature	T_{eff}	6450 ± 50	K
<i>MCMC parameters controlled by Gaussian priors</i>			
Stellar mass	M_*	1.303 ± 0.072	M_\odot
Stellar effective temperature	T_{eff}	6453 ± 49	K
<i>MCMC fitted parameters</i>			
Orbital period	P	4.5111204 ± 0.0000018	d
Transit epoch (HJD)	T_c	$2457501.99114 \pm 0.00050$	d
Transit duration	T_{14}	0.1944 ± 0.0016	d
Planet-to-star area ratio	R_p^2/R_*^2	0.00952 ± 0.00017	...
Impact parameter ^a	b	0.317 ± 0.089	...
Reflex velocity semi-amplitude	K_1	69.1 ± 8.9	m s^{-1}
Systemic velocity (CORALIE)	γ_{CORALIE}	$-26\,355 \pm 12$	m s^{-1}
Systemic velocity (HARPS, RM)	$\gamma_{\text{HARPS, RM}}$	$-26\,360.9 \pm 3.5$	m s^{-1}
Systemic velocity (HARPS, HAM)	$\gamma_{\text{HARPS, HAM}}$	$-26\,361.7 \pm 8.1$	m s^{-1}
Systemic velocity (HARPS, EGGS)	$\gamma_{\text{HARPS, EGGS}}$	$-26\,402 \pm 15$	m s^{-1}
Orbital eccentricity	e	0 (assumed; < 0.14 at 2σ)	...
<i>MCMC derived parameters</i>			
Sky-projected stellar obliquity	λ_{RM}	-19.0 ± 6.1	$^\circ$
Sky-projected stellar rotation speed	$v \sin i_{*, \text{RM}}$	18.9 ± 1.1	km s^{-1}
Scaled semi-major axis	a/R_*	7.77 ± 0.24	...
Orbital inclination	i	87.66 ± 0.73	$^\circ$
Ingress and egress duration	$T_{12} = T_{34}$	0.0190 ± 0.0013	d
Stellar radius	R_*	1.619 ± 0.058	R_\odot
Stellar surface gravity	$\log g_*$	4.135 ± 0.028	[cgs]
Stellar density	ρ_*	0.309 ± 0.028	ρ_\odot
Planetary mass	M_p	0.670 ± 0.089	M_{Jup}
Planetary radius	R_p	1.536 ± 0.062	R_{Jup}
Planetary surface gravity	$\log g_p$	2.810 ± 0.068	[cgs]
Planetary density	ρ_p	0.183 ± 0.033	ρ_J
Orbital semi-major axis	a	0.0584 ± 0.0011	AU
Planetary equilibrium temperature ^b	T_{eq}	1638 ± 29	K
<i>Parameters from a separate MCMC including Doppler tomography</i>			
Sky-projected stellar obliquity	λ_{DT}	-11.3 ± 4.8	$^\circ$
Sky-projected stellar rotation speed	$v \sin i_{*, \text{DT}}$	15.91 ± 0.49	km s^{-1}
Intrinsic linewidth	v_{FWHM}	8.98 ± 0.32	km s^{-1}
Impact parameter	b_{DT}	0.206 ± 0.080	...
Systemic velocity	γ_{DT}	$-27\,520 \pm 400$	m s^{-1}

^aImpact parameter is the distance between the centre of the stellar disc and the transit chord:
 $b = a \cos i/R_*$.

^bEquilibrium temperature calculated assuming zero albedo and efficient redistribution of heat from the planet's presumed permanent day-side to its night-side.

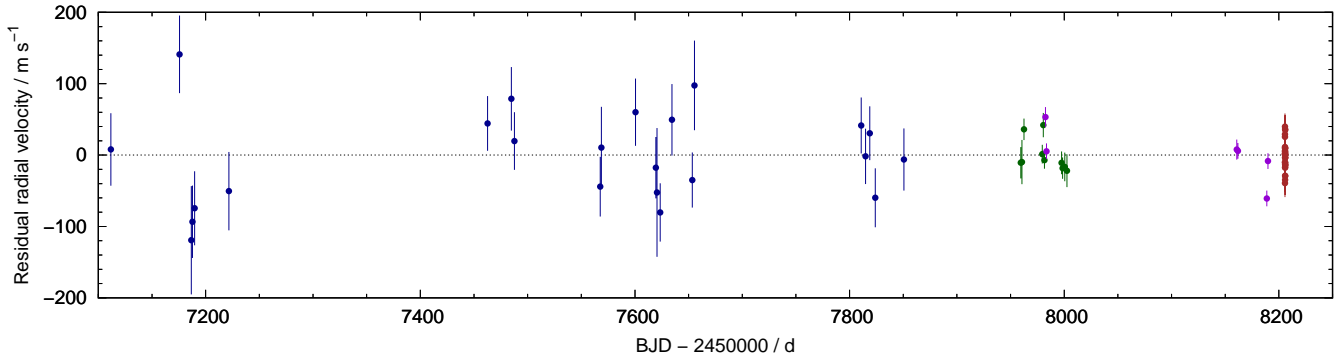


Figure 5. The residual RVs about the best-fitting Keplerian orbital and RM effect models. The symbol colours are the same as in Fig. 1.

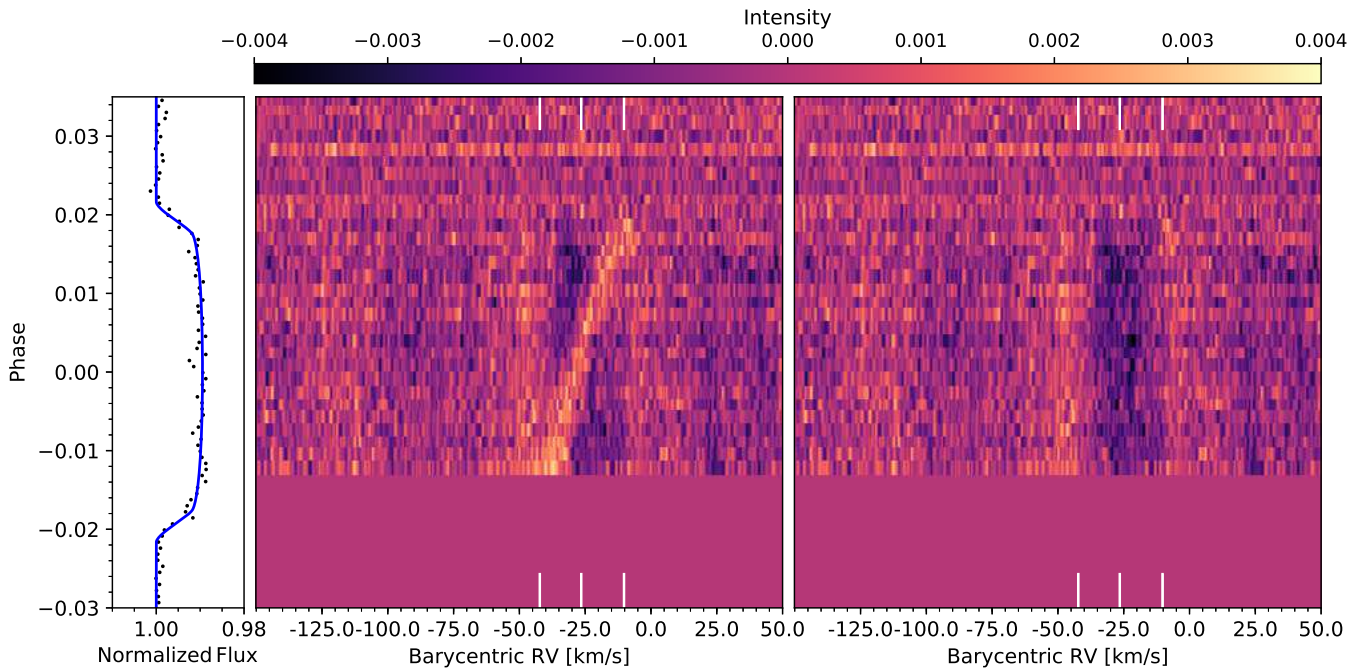


Figure 6. Doppler tomogram of the HARPS spectra taken through a transit of WASP-179b. *Left panel:* The three TRAPPIST transit lightcurves combined, phase-folded on the ephemeris from Table 5, and binned with a bin width equivalent to 5 min. This indicates the timing of the transit for comparison with the tomogram. *Middle panel:* Tomogram of the residuals obtained by subtracting the average of the out-of-transit CCFs from all CCFs, leaving the bright signature of the starlight blocked by the planet during transit. Wavelength or RV increases from left to right, time increases from bottom to top. The white, vertical lines mark the positions of the systemic velocity (γ_{DT}) and the limits of the stellar rotation speed ($\gamma_{DT} \pm v_* \sin i_{*,DT}$). The stellar velocity of the planet trace moves from blue-shifted to red-shifted and covers the full range of stellar rotation, indicating a prograde, near-aligned orbit. *Right panel:* The residual tomogram after subtraction of the planet model.

tude). Whilst we both measured ρ_* from our respective transit lightcurves, we derived R_* from ρ_* and M_* (obtained from stellar models), whereas R18 derived M_* from ρ_* and R_* (obtained from SED fitting and the Gaia parallax). Our values of M_* ($1.30 \pm 0.07 M_\odot$) and R_* ($1.62 \pm 0.06 R_\odot$) are in good agreement both with the values obtained by R18 from stellar models ($M_* = 1.32 \pm 0.09 M_\odot$ and $R_* = 1.58 \pm 0.22 R_\odot$) and the values we obtain from the empirical calibrations of Southworth (2011): $M_* = 1.34 M_\odot$ and $R_* = 1.63 R_\odot$. Further, our value of M_* is consistent with the F5V spectral type that we obtained using the MKCLASS spectral classification code of Gray & Corbally (2014). We note that the discrepancy is not large: the two M_* values agree at the $1.5\text{-}\sigma$ level. This small discrepancy is somewhat due to the difference in stellar density measured from the transit lightcurves (we found $\rho_* = 0.31 \pm 0.03 \rho_\odot$ and R18 found $\rho_* = 0.33 \pm 0.05 \rho_\odot$), but it is more so due to R18's larger stellar radius. R18 obtained $R_* = 1.70 \pm 0.05 R_\odot$ from SED fitting and the Gaia parallax, whereas we obtained $R_* = 1.62 \pm 0.09 R_\odot$ using a similar method, and we derived $R_* = 1.62 \pm 0.06 R_\odot$ from our ρ_* and M_* values. Thus we find a smaller planetary radius than do R18: $R_p = 1.54 \pm 0.06 R_{\text{Jup}}$ compared to $R_p = 1.60 \pm 0.05 R_{\text{Jup}}$ (the difference is slightly smaller than suggested by R_* as we measured a slightly larger planet-to-star area ratio).

Due to the 12-yr baseline (2006-2018) of our transit observations, our ephemeris is considerably more precise than

that of R18 (8-month baseline). Our error bars on the orbital period and on the time of mid-transit are smaller than those of R18 by factors of 34 and 3, respectively.

WASP-South is hosted by the South African Astronomical Observatory; we are grateful for their ongoing support and assistance. Funding for SuperWASP comes from consortium universities and from the UK's Science and Technology Facilities Council. The Swiss *Euler* Telescope is operated by the University of Geneva, and is funded by the Swiss National Science Foundation. The research leading to these results has received funding from the ARC grant for Concerted Research Actions, financed by the Wallonia-Brussels Federation. TRAPPIST is funded by the Belgian Fund for Scientific Research (Fond National de la Recherche Scientifique, FNRS) under the grant FRFC 2.5.594.09.F, with the participation of the Swiss National Science Foundation (SNF). MG and EJ are FNRS Senior Research Associates. Based on observations collected at the European Organisation for Astronomical Research in the Southern Hemisphere under ESO programmes 099.C-0303(A), 099.C-0898(A) and 0100.C-0847(A).

Facilities: SuperWASP, TRAPPIST, Euler1.2m(CORALIE), ESO:3.6m(HARPS)

REFERENCES

- Albrecht, S., Winn, J. N., Johnson, J. A., et al. 2012, *ApJ*, 757, 18, doi: [10.1088/0004-637X/757/1/18](https://doi.org/10.1088/0004-637X/757/1/18)
- Anderson, D. R., Collier Cameron, A., Gillon, M., et al. 2012, *MNRAS*, 422, 1988, doi: [10.1111/j.1365-2966.2012.20635.x](https://doi.org/10.1111/j.1365-2966.2012.20635.x)
- Anderson, D. R., Collier Cameron, A., Hellier, C., et al. 2015, *A&A*, 575, A61, doi: [10.1051/0004-6361/201423591](https://doi.org/10.1051/0004-6361/201423591)
- Anderson, D. R., Collier Cameron, A., Delrez, L., et al. 2017, *A&A*, 604, A110, doi: [10.1051/0004-6361/201730439](https://doi.org/10.1051/0004-6361/201730439)
- Asplund, M., Grevesse, N., Sauval, A. J., & Scott, P. 2009, *ARA&A*, 47, 481, doi: [10.1146/annurev.astro.46.060407.145222](https://doi.org/10.1146/annurev.astro.46.060407.145222)
- Baranne, A., Queloz, D., Mayor, M., et al. 1996, *A&AS*, 119, 373
- Blackwell, D. E., & Shallis, M. J. 1977, *MNRAS*, 180, 177
- Brown, D. J. A., Collier Cameron, A., Díaz, R. F., et al. 2012, *ApJ*, 760, 139, doi: [10.1088/0004-637X/760/2/139](https://doi.org/10.1088/0004-637X/760/2/139)
- Brown, D. J. A., Triaud, A. H. M. J., Doyle, A. P., et al. 2017, *MNRAS*, 464, 810, doi: [10.1093/mnras/stw2316](https://doi.org/10.1093/mnras/stw2316)
- Bruntt, H., Basu, S., Smalley, B., et al. 2012, *MNRAS*, 423, 122, doi: [10.1111/j.1365-2966.2012.20686.x](https://doi.org/10.1111/j.1365-2966.2012.20686.x)
- Collier Cameron, A., Bruce, V. A., Miller, G. R. M., Triaud, A. H. M. J., & Queloz, D. 2010a, *MNRAS*, 403, 151, doi: [10.1111/j.1365-2966.2009.16131.x](https://doi.org/10.1111/j.1365-2966.2009.16131.x)
- Collier Cameron, A., Pollacco, D., Street, R. A., et al. 2006, *MNRAS*, 373, 799, doi: [10.1111/j.1365-2966.2006.11074.x](https://doi.org/10.1111/j.1365-2966.2006.11074.x)
- Collier Cameron, A., Wilson, D. M., West, R. G., et al. 2007, *MNRAS*, 380, 1230, doi: [10.1111/j.1365-2966.2007.12195.x](https://doi.org/10.1111/j.1365-2966.2007.12195.x)
- Collier Cameron, A., Guenther, E., Smalley, B., et al. 2010b, *MNRAS*, 407, 507, doi: [10.1111/j.1365-2966.2010.16922.x](https://doi.org/10.1111/j.1365-2966.2010.16922.x)
- Dawson, R. I., & Johnson, J. A. 2018, *ArXiv e-prints*, <https://arxiv.org/abs/1801.06117>
- Doyle, A. P., Davies, G. R., Smalley, B., Chaplin, W. J., & Elsworth, Y. 2014, *MNRAS*, 444, 3592, doi: [10.1093/mnras/stu1692](https://doi.org/10.1093/mnras/stu1692)
- Doyle, A. P., Smalley, B., Maxted, P. F. L., et al. 2013, *MNRAS*, 428, 3164, doi: [10.1093/mnras/sts267](https://doi.org/10.1093/mnras/sts267)
- Evans, D. F., Southworth, J., & Smalley, B. 2016, *ApJL*, 833, L19, doi: [10.3847/2041-8213/833/2/L19](https://doi.org/10.3847/2041-8213/833/2/L19)
- Gaia Collaboration, Brown, A. G. A., Vallenari, A., et al. 2018, *A&A*, 616, A1, doi: [10.1051/0004-6361/201833051](https://doi.org/10.1051/0004-6361/201833051)
- Gillon, M., Jehin, E., Magain, P., et al. 2011, *Detection and Dynamics of Transiting Exoplanets*, St. Michel l'Observatoire, France, Edited by F. Bouchy; R. Díaz; C. Moutou; EPJ Web of Conferences, Volume 11, id.06002, 11, 6002, doi: [10.1051/epjconf/20101106002](https://doi.org/10.1051/epjconf/20101106002)

- Gray, R. O., & Corbally, C. J. 2014, *AJ*, 147, 80, doi: [10.1088/0004-6256/147/4/80](https://doi.org/10.1088/0004-6256/147/4/80)
- Günther, M. N., Queloz, D., Gillen, E., et al. 2018, *MNRAS*, 478, 4720, doi: [10.1093/mnras/sty1193](https://doi.org/10.1093/mnras/sty1193)
- Hellier, C., Anderson, D. R., Cameron, A. C., et al. 2017, *MNRAS*, 465, 3693, doi: [10.1093/mnras/stw3005](https://doi.org/10.1093/mnras/stw3005)
- Hirano, T., Suto, Y., Winn, J. N., et al. 2011, *ApJ*, 742, 69, doi: [10.1088/0004-637X/742/2/69](https://doi.org/10.1088/0004-637X/742/2/69)
- Jackson, B., Greenberg, R., & Barnes, R. 2008, *ApJ*, 678, 1396, doi: [10.1086/529187](https://doi.org/10.1086/529187)
- Jehin, E., Gillon, M., Queloz, D., et al. 2011, *The Messenger*, 145, 2
- Jenkins, J. M., Borucki, W. J., Koch, D. G., et al. 2010, *ApJ*, 724, 1108, doi: [10.1088/0004-637X/724/2/1108](https://doi.org/10.1088/0004-637X/724/2/1108)
- Kreidberg, L., Line, M. R., Thorngren, D., Morley, C. V., & Stevenson, K. B. 2018, *ApJL*, 858, L6, doi: [10.3847/2041-8213/aabfce](https://doi.org/10.3847/2041-8213/aabfce)
- Labadie-Bartz, J., Rodriguez, J. E., Stassun, K. G., et al. 2018, ArXiv e-prints. <https://arxiv.org/abs/1803.07559>
- Maxted, P. F. L., Serenelli, A. M., & Southworth, J. 2015, *A&A*, 575, A36, doi: [10.1051/0004-6361/201425331](https://doi.org/10.1051/0004-6361/201425331)
- Maxted, P. F. L., Anderson, D. R., Collier Cameron, A., et al. 2011, *PASP*, 123, 547, doi: [10.1086/660007](https://doi.org/10.1086/660007)
- Pepe, F., Mayor, M., Rupprecht, G., et al. 2002, *The Messenger*, 110, 9
- Petrovich, C. 2015, *ApJ*, 805, 75, doi: [10.1088/0004-637X/805/1/75](https://doi.org/10.1088/0004-637X/805/1/75)
- Pollacco, D. L., Skillen, I., Cameron, A. C., et al. 2006, *PASP*, 118, 1407, doi: [10.1086/508556](https://doi.org/10.1086/508556)
- Queloz, D., Mayor, M., Weber, L., et al. 2000, *A&A*, 354, 99
- Queloz, D., Henry, G. W., Sivan, J. P., et al. 2001, *A&A*, 379, 279, doi: [10.1051/0004-6361:20011308](https://doi.org/10.1051/0004-6361:20011308)
- Raynard, L., Goad, M. R., Gillen, E., et al. 2018, ArXiv e-prints. <https://arxiv.org/abs/1805.10449>
- Schlafly, E. F., & Finkbeiner, D. P. 2011, *ApJ*, 737, 103, doi: [10.1088/0004-637X/737/2/103](https://doi.org/10.1088/0004-637X/737/2/103)
- Southworth, J. 2011, *MNRAS*, 417, 2166, doi: [10.1111/j.1365-2966.2011.19399.x](https://doi.org/10.1111/j.1365-2966.2011.19399.x)
- Spake, J. J., Sing, D. K., Evans, T. M., et al. 2018, *Nature*, 557, 68, doi: [10.1038/s41586-018-0067-5](https://doi.org/10.1038/s41586-018-0067-5)
- Stassun, K. G., & Torres, G. 2018, *ApJ*, 862, 61, doi: [10.3847/1538-4357/aaca6c](https://doi.org/10.3847/1538-4357/aaca6c)
- Temple, L. Y., Hellier, C., Albrow, M. D., et al. 2017, *MNRAS*, 471, 2743, doi: [10.1093/mnras/stx1729](https://doi.org/10.1093/mnras/stx1729)
- Temple, L. Y., Hellier, C., Almléaky, Y., et al. 2018, *MNRAS*, 480, 5307, doi: [10.1093/mnras/sty2197](https://doi.org/10.1093/mnras/sty2197)
- Torres, G., Konacki, M., Sasselov, D. D., & Jha, S. 2004, *ApJ*, 614, 979, doi: [10.1086/423734](https://doi.org/10.1086/423734)
- Wheatley, P. J., West, R. G., Goad, M. R., et al. 2018, *MNRAS*, 475, 4476, doi: [10.1093/mnras/stx2836](https://doi.org/10.1093/mnras/stx2836)
- Wyttenbach, A., Lovis, C., Ehrenreich, D., et al. 2017, *A&A*, 602, A36, doi: [10.1051/0004-6361/201630063](https://doi.org/10.1051/0004-6361/201630063)